

Dynamic Behavior of Avian Influenza A Virus Neuraminidase Subtype H5N1 in Complex with Oseltamivir, Zanamivir, Peramivir, and Their Phosphonate Analogues

Thanyarat Udommaneethanakit,^{†,‡,§} Thanyada Rungrotmongkol,^{†,‡,||} Urban Bren,^{†,‡,⊥}
Vladimir Frečer,^{‡,¶} and Miertus Stanislav^{*,‡}

International Centre for Science and High Technology, UNIDO, AREA Science Park, Padriciano 99, I-34012 Trieste, Italy, Nanoscience and Technology Program, Graduate School, and Center of Innovative Nanotechnology, Chulalongkorn University, Phayathai Road, Pathumwan, 10330 Bangkok, Thailand, National Institute of Chemistry, Hajdrihova 19, SI-1001 Ljubljana, Slovenia, and Cancer Research Institute, Slovak Academy of Sciences, Vlarska 7, SK-83391 Bratislava, Slovakia

Received July 29, 2009

The outbreak of avian influenza A subtype H5N1 virus has raised a global concern for both animal as well as human health. Recently, drug resistance in H5N1 infections has been widely reported due to neuraminidase mutations. Consequently, the understanding of inhibitor-neuraminidase interactions at the molecular level represents the main goal of our study. Molecular dynamics simulations were carried out for the neuraminidase N1 in complex with six inhibitors - oseltamivir, zanamivir, peramivir, and their phosphonate analogues. Molecular dynamics trajectories were extensively analyzed in terms of important interactions between inhibitors and the enzyme target. Results show that open and closed forms (defined by the relative position of the flexible 150-loop) of neuraminidase N1 interchange during the course of 20 ns molecular dynamics simulation of the protein-inhibitor complexes. Reported free energies of closing indicate that the carboxylate inhibitors prefer the closed form more than their phosphonate analogues. This can be understood in view of the negative total charge ($-1\ e_0$) of the phosphonate inhibitors, which repels the Asp151 residue of the loop away from the inhibitor and drives the complex into the open form. Obtained results constitute new valuable information to assist further drug development of inhibitors against the H5N1 avian influenza A virus and could also inspire similar studies for other systems of the influenza family such as the 2009 influenza A (H1N1) virus.

1. INTRODUCTION

The outbreak of avian influenza A virus subtype H5N1 has raised a global concern for both animal as well as human health due to the possibility of an antigenic shift allowing for human-to-human transmission. The classification of influenza A virus subtypes is based on the antigenic properties of its surface glycoproteins hemagglutinin (H1–H16) and neuraminidase (N1–N9) both of which play essential roles for infection to proceed.¹ While hemagglutinin is important for attachment to the glycans containing the terminal sialic acid on the surface of epithelial cells, allowing for penetration into the host cell, neuraminidase cleaves the linkage formed between the hemagglutinin and sialic acid when mature viruses detach from the host cell surface.² Several anti-influenza drugs targeting the neuraminidase inhibit cleavage of terminal sialic acid and suppress the release of progeny viruses from infected cells.³ The first designed neuraminidase inhibitor zanamivir is available under the commercial name of Relenza and is administered through

inhalation.⁴ Subsequent discovery of oseltamivir provided the first orally available neuraminidase inhibitor which is known under the brand name of Tamiflu.⁵ Peramivir - the third neuraminidase inhibitor - displays only limited oral bioavailability.^{6,7} Intravenous peramivir is currently undergoing a pre-emergency use authorization review for the use in cases of severe influenza outbreaks. Neuraminidase remains an attractive anti-influenza drug target, not least because of the emergence of viruses resistant to the currently available drugs.^{8–11} Recently, phosphonate congeners of oseltamivir and its analogs have been shown to possess higher binding affinity toward neuraminidase N1 of avian influenza A virus.¹²

Upon binding of substrates or inhibitors to the neuraminidase N1, the binding pocket undergoes significant rearrangement of the so-called 150-loop (residues 147–152).¹³ In the apo structure the loop occupies an ‘open’ conformation which exposes a larger active-site cavity. On the other hand, in the complex with oseltamivir the 150-loop eventually closes to tightly coordinate the inhibitor. Surprisingly, crystal structures of neuraminidase N1 reveal that the enzyme is under specific soaking conditions able to bind oseltamivir also in the open conformation of the 150-loop.¹³ Therefore, understanding of the role of the flexible 150-loop upon inhibitor binding to neuraminidase N1 represents a new opportunity for rational drug design. Differences between crystal structures of the open and closed forms of neuraminidase N1

* Corresponding author fax: (+39-040) 922 8115; e-mail: stanislav.miertus@ics.trieste.it.

[†] These authors contributed equally to this work.

[‡] International Centre for Science and High Technology, UNIDO.

[§] Nanoscience and Technology Program, Graduate School, Chulalongkorn University.

^{||} Center of Innovative Nanotechnology, Chulalongkorn University.

[⊥] National Institute of Chemistry.

[¶] Slovak Academy of Sciences.

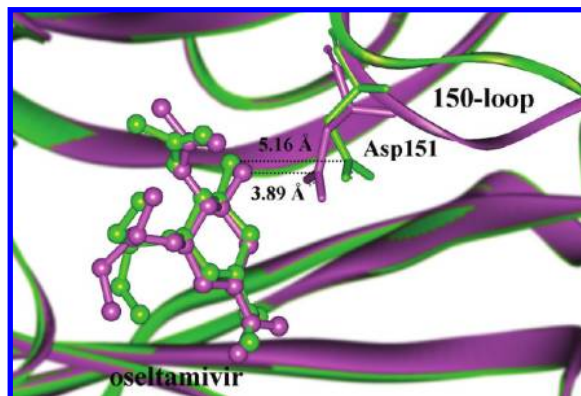


Figure 1. Structural alignment between crystal structures of neuraminidase N1 in closed (violet ribbons) and open (green ribbons) conformations complexed with oseltamivir (OTV). Close-up of oseltamivir, Asp151, and the 150-loop depicts the distance between the N4 atom of oseltamivir and the CG carbon of Asp151.

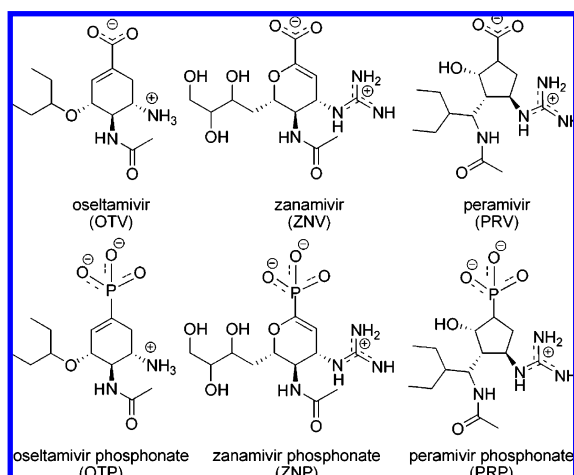


Figure 2. Chemical structures of the studied neuraminidase inhibitors: oseltamivir (OTV), zanamivir (ZNV), peramivir (PRV), and their phosphonate analogues (OTP, ZNP, and PRP).

(PDB entry codes 2HU0 and 2HU4, respectively)¹³ are shown in Figure 1. The distance between N4 atom of oseltamivir and CG atom of Asp151 is about 5.2 Å in the open and 3.9 Å in the closed conformations of the 150-loop, respectively. Finally, molecular dynamics simulations revealed that the 150-loop switching motion is able to open also a significantly wider binding pocket of neuraminidase N1 than the ones observed in the crystal structures.^{14,15}

In this study, molecular dynamics (MD) simulations of neuraminidase N1 in complex with six different ligands depicted in Figure 2 - oseltamivir (OTV), oseltamivir phosphonate (OTP), zanamivir (ZNV), zanamivir phosphonate (ZNP), peramivir (PRV), and peramivir phosphonate (PRP) - were performed. The main goal was to analyze important interactions between each of the six inhibitors and the enzyme target as well as to understand the 150-loop flexibility and related open and closed conformations of the six inhibitor-enzyme complexes. These results constitute new valuable information to assist further drug design efforts toward inhibition of the H5N1 avian influenza A virus as well as the 2009 H1N1 influenza A virus since they belong to the same neuraminidase subtype.

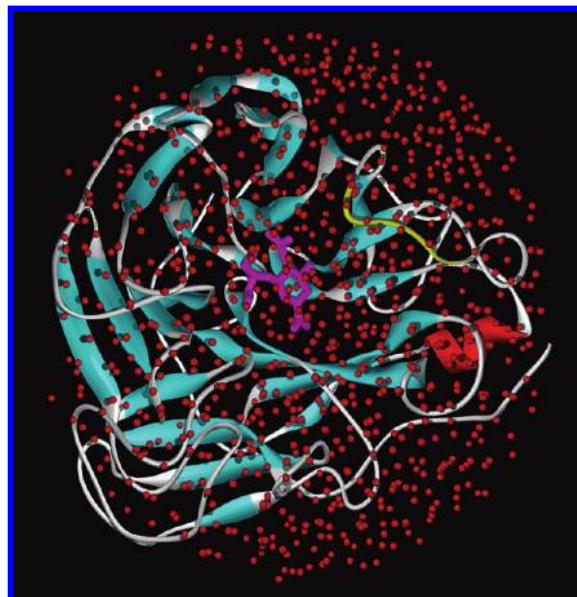


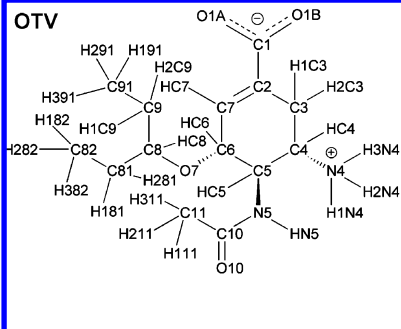
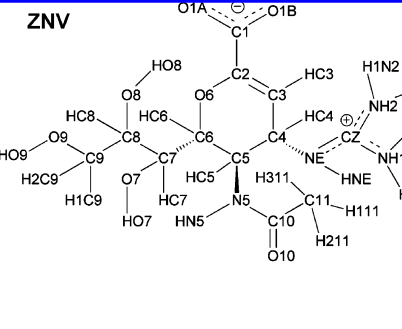
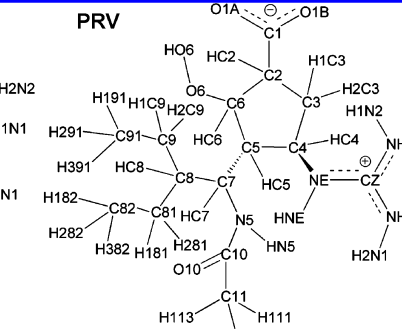
Figure 3. Initial structure of the neuraminidase N1 in the open conformation complexed with oseltamivir. The flexible 150-loop is depicted in yellow, and the red balls represent water molecules.

2. COMPUTATIONAL METHODS

2.1. Initial Structure Preparation. Experimentally solved 3D-structures of neuraminidase N1 in the open and closed conformations cocrystallized with oseltamivir (OTV-N1), which represent the starting coordinates for our molecular dynamics simulations, were retrieved from the Protein Data Bank (PDB entry codes 2HU0 and 2HU4, respectively).¹³ Structures of zanamivir (ZNV) and peramivir (PRV) were extracted from their crystal complexes with neuraminidase N8 (PDB entry codes 2HTQ and 2HTU, respectively).¹³ To prepare ZNV-N1 and PRV-N1 structures, superposition of the two inhibitors over the selected heavy atoms of oseltamivir in complex with the open and closed conformation of neuraminidase N1 was performed, and oseltamivir atoms were subsequently removed. Russell et al.¹³ observed that the structures of N1 and N8 subtypes are very similar after inhibitor binding and that the inhibitors share about the same binding mode in both neuraminidase subtypes. The phosphonate analogues complexed with the open and closed conformations of neuraminidase N1 (OTP-N1, ZNP-N1, and PRP-N1) were finally constructed by manually replacing the carboxylate group with the phosphonate group. Beowulf-type CROW clusters at the National Institute of Chemistry in Ljubljana, Slovenia, were exploited in our computational studies.^{16,17} Preparation of the initial structures as well as molecular dynamics simulations were performed with the Q program¹⁸ developed by Åqvist and co-workers using the AMBER force field.¹⁹

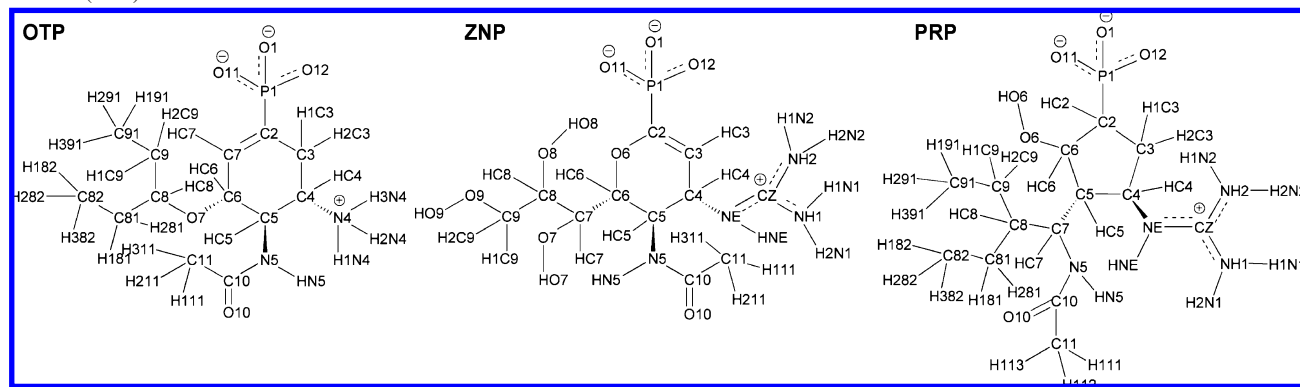
All crystal waters were deleted, and each inhibitor-enzyme complex was solvated by a 24 Å radius sphere of TIP3P²⁰ water molecules centered on the C2 atom of the inhibitor. Water molecules that sterically overlapped with the atoms in the crystal structure were deleted. Protonation of the ionizable amino acid residues was assigned by the following rules: side chains of Asp and Glu residues located within 21 Å of the sphere center were considered negatively charged. Similarly, side chains of Lys and Arg residues were treated as positively charged. In the area between 21 Å and 24 Å

Table 1. Atom Names, Atom Types, and Partial Atomic Charges of Oseltamivir (OTV), Zanamivir (ZNV), and Peramivir (PRV)

OTV			ZNV			PRV		
								
name	type	q	name	type	q	name	type	q
C1	C	0.7820	C1	C	0.8107	C4	CT	0.1087
O1A	O2	-0.7511	O1A	O2	-0.7323	HC4	HC	0.0899
O1B	O2	-0.7511	O1B	O2	-0.7323	NE	N2	-0.4954
C2	CM	-0.0362	C2	CM	0.0684	HNE	H	0.2981
C3	CT	-0.0284	C3	CM	-0.4181	CZ	CA	0.7278
H1C3	HC	0.0477	HC3	HA	0.1765	NH1	N2	-0.8287
H2C3	HC	0.0477	C4	CT	-0.0063	H1N1	H	0.4037
C4	CT	0.1193	HC4	HC	0.0998	H2N1	H	0.4037
HC4	HC	0.1064	C5	CT	0.3666	NH2	N2	-0.8287
C5	CT	-0.0078	HC5	HC	0.1193	H1N2	H	0.4034
HC5	HC	0.1303	N5	N	-0.6697	H2N2	H	0.4034
N5	N	-0.3088	HN5	H	0.3048	C5	CT	-0.0141
HN5	H	0.1142	C10	C	0.7262	HC5	HC	0.0959
C10	C	0.6342	O10	O	-0.5921	C7	CT	0.0134
O10	O	-0.6246	C11	CT	-0.3741	HC7	HC	0.1523
C11	CT	-0.2981	H111	HC	0.1194	C8	CT	-0.0083
H111	HC	0.1075	H211	HC	0.1194	HC8	HC	0.0903
H211	HC	0.1075	H311	HC	0.1194	C9	CT	-0.0172
H311	HC	0.1075	C6	CT	0.0153	H1C9	HC	0.0225
C6	CT	-0.0180	HC6	HC	0.0516	H2C9	HC	0.0225
HC6	HC	0.1074	O6	OS	-0.1499	C91	CT	-0.1501
C7	CM	-0.3125	C7	CT	-0.0028	H191	HC	0.0406
HC7	HA	0.2184	HC7	H1	0.1361	H291	HC	0.0406
O7	OS	-0.2300	O7	OH	-0.6278	H391	HC	0.0406
C8	CT	0.0094	HO7	HO	0.4264	C81	CT	-0.0172
HC8	HC	0.0513	C8	CT	0.1556	H181	HC	0.0225
C9	CT	0.0152	HC8	H1	0.0647	H182	HC	0.0225
H1C9	HC	0.0277	O8	OH	-0.6573	C82	CT	-0.1501
H2C9	HC	0.0277	HO8	HO	0.4434	H182	HC	0.0406
C81	CT	0.0152	C9	CT	0.1631	H282	HC	0.0406
H181	HC	0.0277	H1C9	H1	0.0276	H382	HC	0.0406
H281	HC	0.0277	H2C9	H1	0.0276	N5	N	-0.5716
C82	CT	-0.1153	O9	OH	-0.6307	HN5	H	0.2888
H182	HC	0.0375	HO9	HO	0.4162	C10	C	0.7505
H282	HC	0.0375	NE	N2	-0.3515	C11	CT	-0.3889
H382	HC	0.0375	HNE	H	0.2348	H111	HC	0.1109
C91	CT	-0.1153	CZ	CA	0.7636	H112	HC	0.1109
H191	HC	0.0375	NH1	N2	-0.8824	H113	HC	0.1109
H291	HC	0.0375	H1N1	H	0.4383	O10	O	-0.6358
H391	HC	0.0375	H2N1	H	0.4383	C6	CT	0.0131
N4	N3	-0.3241	NH2	N2	-0.8824	HC6	H1	0.1239
H1N4	H	0.2881	H1N2	H	0.4383	O6	OH	-0.6884
H2N4	H	0.2881	H2N2	H	0.4383	HO6	HO	0.4518
H3N4	H	0.2881				C2	CT	-0.0265
						HC2	HC	0.0354
						C1	C	0.7139
						O1B	O2	-0.7164
						O1A	O2	-0.7164
						C3	CT	-0.0593
						H1C3	HC	0.0394
						H2C3	HC	0.0394

away from the sphere center, the ionizable residues were generally considered neutral entities. In the case of an identified salt bridge, both of the interacting partners

remained charged. Histidine residues located within 21 Å of the sphere center were assigned their protonation pattern in the last stage to approach the electroneutrality of the

Table 2. Atom Names, Atom Types, and Partial Atomic Charges of the Phosphonate Analogues of Oseltamivir (OTP), Zanamivir (ZNP), and Peramivir (PRP)

OTP			ZNP			PRP		
name	type	q	name	type	q	name	type	q
P1	P	1.2279	P1	P	1.2592	C4	CT	0.1087
O11	O2	-0.9422	O11	O2	-0.9544	HC4	HC	0.0899
O12	O2	-0.9422	O12	O2	-0.9544	NE	N2	-0.4954
C2	CM	0.1343	C2	CM	0.2379	HNE	H	0.2981
C3	CT	-0.158	C3	CM	-0.5638	CZ	CA	0.7278
H1C3	HC	0.0477	HC3	HA	0.2154	NH1	N2	-0.8287
H2C3	HC	0.0477	C4	CT	-0.0063	H1N1	H	0.4037
C4	CT	0.1193	HC4	HC	0.0998	H2N1	H	0.4037
HC4	HC	0.1064	C5	CT	0.3666	NH2	N2	-0.8287
C5	CT	-0.0078	HC5	HC	0.1193	H1N2	H	0.4034
HC5	HC	0.1303	N5	N	-0.6697	H2N2	H	0.4034
N5	N	-0.3088	HN5	H	0.3048	C5	CT	-0.0141
HN5	H	0.1142	C10	C	0.7262	HC5	HC	0.0959
C10	C	0.6342	O10	O	-0.5921	C7	CT	0.0134
O10	O	-0.6246	C11	CT	-0.3741	HC7	HC	0.1523
C11	CT	-0.2981	H111	HC	0.1194	C8	CT	-0.0083
H111	HC	0.1075	H211	HC	0.1194	HC8	HC	0.0903
H211	HC	0.1075	H311	HC	0.1194	C9	CT	-0.0172
H311	HC	0.1075	C6	CT	0.0153	H1C9	HC	0.0225
C6	CT	-0.018	HC6	HC	0.0516	H2C9	HC	0.0225
HC6	HC	0.1074	O6	OS	-0.2625	C91	CT	-0.1501
C7	CM	-0.4749	C7	CT	-0.0028	H191	HC	0.0406
HC7	HA	0.2184	HC7	H1	0.1361	H291	HC	0.0406
O7	OS	-0.23	O7	OH	-0.6278	H391	HC	0.0406
C8	CT	0.0094	HO7	HO	0.4264	C81	CT	-0.0172
HC8	HC	0.0513	C8	CT	0.1556	H181	HC	0.0225
C9	CT	0.0152	HC8	H1	0.0647	H182	HC	0.0225
H1C9	HC	0.0277	O8	OH	-0.6573	C82	CT	-0.1501
H2C9	HC	0.0277	HO8	HO	0.4434	H182	HC	0.0406
C81	CT	0.0152	C9	CT	0.1631	H282	HC	0.0406
H181	HC	0.0277	H1C9	H1	0.0276	H382	HC	0.0406
H281	HC	0.0277	H2C9	H1	0.0276	N5	N	-0.5716
C82	CT	-0.1153	O9	OH	-0.6307	HN5	H	0.2888
H182	HC	0.0375	HO9	HO	0.4162	C10	C	0.7505
H282	HC	0.0375	NE	N2	-0.3515	C11	CT	-0.3889
H382	HC	0.0375	HNE	H	0.2348	H111	HC	0.1109
C91	CT	-0.1153	CZ	CA	0.7636	H112	HC	0.1109
H191	HC	0.0375	NH1	N2	-0.8824	H113	HC	0.1109
H291	HC	0.0375	H1N1	H	0.4383	O10	O	-0.6358
H391	HC	0.0375	H2N1	H	0.4383	C6	CT	0.0131
N4	N3	-0.3241	NH2	N2	-0.8824	HC6	H1	0.1239
H1N4	H	0.2881	H1N2	H	0.4383	O6	OH	-0.7098
H2N4	H	0.2881	H2N2	H	0.4383	HO6	HO	0.4304
H3N4	H	0.2881	O1	O2	-0.9544	C2	CT	-0.0265
O1	O2	-0.9422				HC2	HC	0.0354
						P1	P	1.1607
						O11	O2	-0.9456
						O12	O2	-0.9456
						C3	CT	-0.0593
						H1C3	HC	0.0394
						H2C3	HC	0.0394
						O1	O2	-0.9456

system as closely as possible. All ionizable side chains outside of the simulation sphere were modeled as uncharged entities. In our MD simulations, the following residues were considered charged: Arg (118, 152, 156, 224, 292, 300, 327, 364, 371, 428, 430), Lys (150, 350, 432), Asp (103, 151, 198, 243, 293, 324, 330, 460), Glu (119, 227, 229, 276, 277, 375, 425, 433), and His (155, 274, 296). Altogether, a net charge of +1 was obtained for the OTV-N1, ZNV-N1, and PRV-N1 systems and was subsequently neutralized by addition of a chloride ion between 5 Å and 7 Å away from the simulation sphere center, while a neutral net charge was found in the case of the three phosphonate analogues. The initial structure of the neuraminidase N1 in the open conformation complexed with oseltamivir is depicted in Figure 3.

2.2. Molecular Dynamics Simulations. The systems were subjected to Surface Constraint All Atoms Solvent (SCAAS) spherical boundary conditions, which mimic the infinite aqueous solution.²¹ Protein atoms protruding beyond the 24 Å sphere boundary were restrained to their coordinates from the crystal structure using harmonic constraints. Nonbonding interactions of these atoms were turned off. Other nonbonding interactions were explicitly evaluated for distances under 10 Å. The Local Reaction Field (LRF) method was used to treat long-range electrostatics for distances beyond the 10 Å cutoff.²² The position of the chloride ion was restrained by a 75 kcal/(mol Å²) flat-bottom harmonic potential that was set to zero for distances less than 20.5 Å from the center of the simulation sphere. This potential was applied to prevent diffusion of the chloride ion toward the edge of the simulation sphere.

All systems were first optimized by 30000- and 20000-step MD simulations at 5 K with a step size of 0.005 and 0.01 fs, respectively. Coordinates of protein and ligand heavy atoms were constrained, allowing only for water relaxation. In further stages the whole system was relaxed at 5 K by a series of four 20000- and one 50000-step simulations with increasing step size (step size prolongation program: 0.01 fs, 0.04 fs, 0.1 fs, 0.3 fs, and 1 fs). Subsequent heating of the simulated system from 5 to 298 K was performed by a series of six MD simulations with a 1 fs step size (temperature heating program: 50 K, 100 K, 150 K, 200 K, 250 K, and 298 K), comprising 300 ps of total simulation time. A 200 ps MD simulation at 298 K using a 2 fs step size with the SHAKE algorithm^{23,24} applied to bonds involving hydrogen atoms yielded the starting structure for the production phase.

Twenty ns production trajectories generated (N, V, T) ensembles at 298 K for each of the twelve investigated systems. The integration step was 2 fs, and the SHAKE algorithm was applied to bonds involving hydrogen atoms. Visualization and analysis of production trajectories were performed using the VMD 1.8.6 program.²⁵

3. RESULTS AND DISCUSSION

3.1. Development of Empirical Force Field Parameters.

Empirical force field parameters of the carboxylate compounds OTV, ZNV, and PRV were developed in the following way. (i) Hydrogen atoms were added to the X-ray structures of the three ligands by taking into consideration the hybridization of the covalent bonds. (ii)

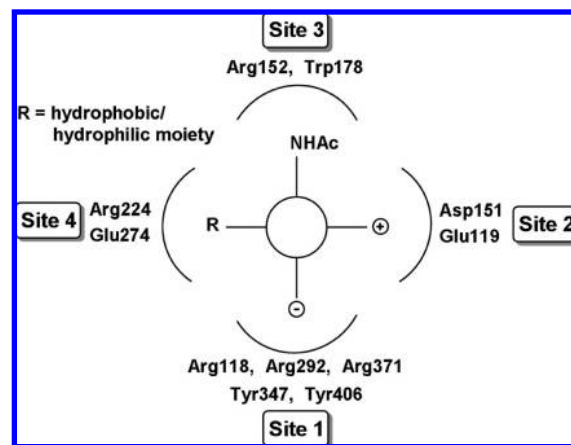


Figure 4. Schematic representation of an inhibitor in the neuraminidase N1 binding site.

Obtained structures were subjected to full geometry optimization and subsequent vibrational analysis in the harmonic approximation at the Hartree–Fock (HF) level of theory using 6-31G(d) basis set encoded in the Gaussian 03 program.²⁶ The absence of imaginary vibrational frequencies indicated correctly performed minimizations.²⁷ (iii) The RESP charge-fitting procedure was initiated to reproduce the HF/6-31G(d) calculated electrostatic potential (ESP) surrounding the inhibitors.²⁸ Partial charges of chemically equivalent atoms were restricted to the same value. (iv) Standard van der Waals parameters were applied due to sufficient transferability between molecules. Missing stretching, bending, dihedral, and improper dihedral parameters required for the complete description of the inhibitors were taken from the Generalized AMBER Force Field (GAFF).²⁹ Force field parameters of the phosphonate group of the phosphonate congeners OTP, ZNP, and PRP were developed using identical procedure. Atom names, atom types, and partial atomic charges of the six neuraminidase inhibitors are presented in Tables 1 and 2.

3.2. Important Interactions. Figure 4 shows a generalized inhibitor in the neuraminidase N1 binding site. The circle represents a six- (OTV, OTP, ZNV, and ZNP) or five- (PRV and PRP) membered ring of the inhibitor and each arm one substituent. The negative arm stands for the carboxylate group of OTV, ZNV, or PRV as well as for the phosphonate group of OTP, ZNP or PRP. The positive arm denotes the ammonium group of OTV or OTP as well as the guanidinium group of ZNV, ZNP, PRV, or PRP. The third arm represents the acetamide group in all inhibitors, while R stands for the hydrophilic moiety of ZNV or ZNP as well as for the hydrophobic moiety of OTV, OTP, PRV, or PRP. Important interactions of each substituent with the amino acid residues of neuraminidase N1 binding site are also depicted based on the results of the present study.

Figures 5, 6, and 7 depict the time dependence of important interactions between the six studied inhibitors and the amino acid residues of neuraminidase N1 in the open and closed conformations. The negatively charged carboxylate or phosphonate group of all inhibitors interacts strongly with the three conserved arginine residues^{13,30} (Arg118, Arg292, and Arg371) regardless of the neuraminidase N1 conformation. Although the exact identity of the hydrogen bonds may interchange during the course of the

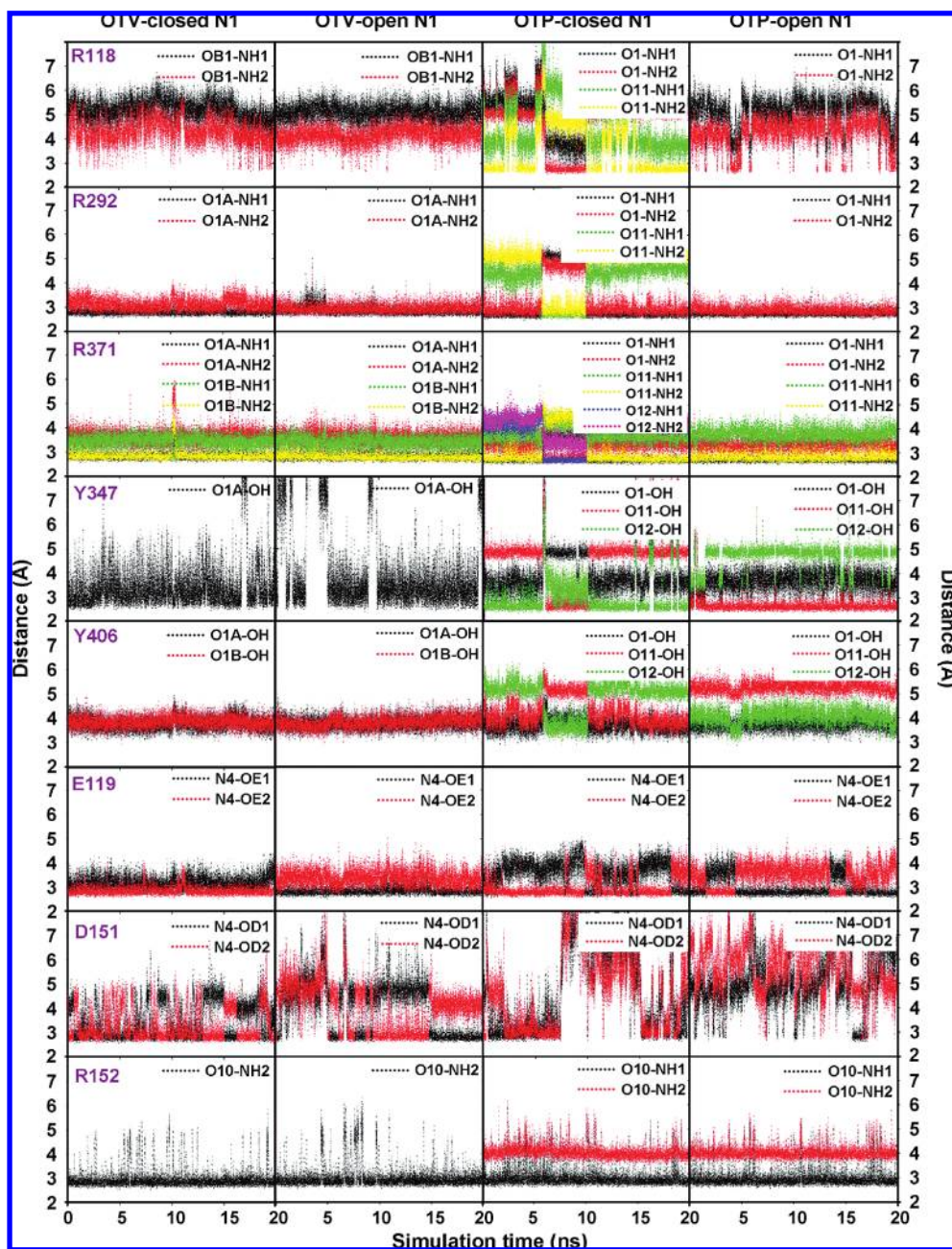


Figure 5. Time dependence of important interactions between neuraminidase N1 amino acid residues and oseltamivir (OTV) or its phosphonate analogue (OTP).

20 ns molecular dynamics trajectory, one can observe two strong hydrogen bonds of the negatively charged group of all inhibitors with both Arg292 and Arg371, while at most one hydrogen bond with Arg118. In contrast to both OTV and PRV where Arg292 interacts firmly with the O1A atom of the carboxylate, the same amino acid residue is less anchored with ZNV, where it samples multiple interaction sites - O1A, O6, and O8 (see footnote of Table 1 for the atomic labels). This might explain why ZNV binding was less affected by the R292K resistant-conferring mutation of neuraminidase N1². Moreover, Tyr347 - a conserved amino acid residue of all group-1 neuraminidases^{13,15} - was found to form a hydrogen bond with the negatively charged substituent of all six inhibitors regardless of the neuraminidase 150-loop conformation as well as occasionally with the O7 atom of ZNV in the closed configuration. Furthermore, Tyr406 interacts with

the negatively charged group of OTV and OTP (consistent with previous studies^{14,31}) as well as occasionally with the negatively charged substituent, the O6 atom, or the positively charged substituent of ZNV, ZNP, PRV, and PRP. Taken together, the phosphonate group was found to interact more firmly with the neighboring amino acid residues than the carboxylate (see R118 and Y347 of Figures 5 and 6 as well as Y347 and Y406 of Figure 7), which can explain why carboxylate inhibitors represent weaker binders of neuraminidase N1 than their phosphonate congeners.¹²

Glu119 in accordance with previous studies^{14,15,31} forms one strong hydrogen bond with the ammonium group of OTV and OTP regardless of the neuraminidase N1 conformation as well as occasionally with the guanidinium group of ZNV, ZNP, PRV, and PRP. Asp151 represents the point of closest approach of the flexible 150-loop to

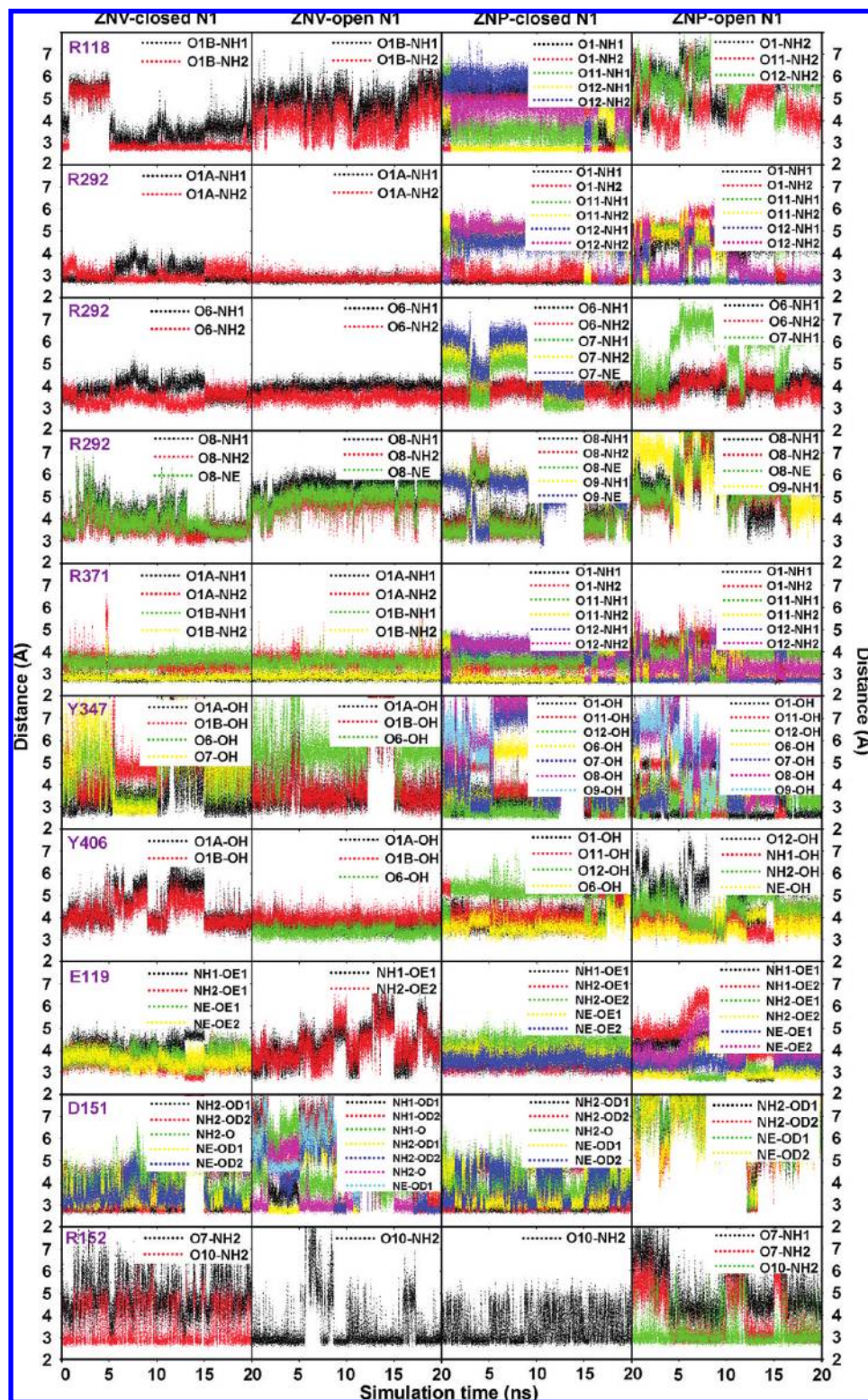


Figure 6. Time dependence of important interactions between neuraminidase N1 amino acid residues and zanamivir (ZNV) or its phosphonate analogue (ZNP).

the enzyme active site.¹³ Position of the Asp151 can be, therefore, used to discriminate between open and closed neuraminidase N1 conformations. Our simulations show that initially closed neuraminidase N1 conformations can lose the hydrogen-bonding interaction of Asp151 with the positively charged group of inhibitors and consequently turn to the open form. Likewise, the initially open neuraminidase N1 conformations can form the hydrogen-bonding interaction between Asp151 and the positively

charged group of inhibitors and consequently close - all within a single 20 ns molecular dynamics trajectory (see D151 of Figures 5, 6, and 7). These findings are in compliance with conclusions of other contemporary studies^{14,15} suggesting that the loop switching motion may be more rapid than previously supposed. PRV and PRP represent the only exception, where Asp151 occasionally forms a hydrogen bond also with the O6 hydroxyl group - consistent with previous studies.³¹

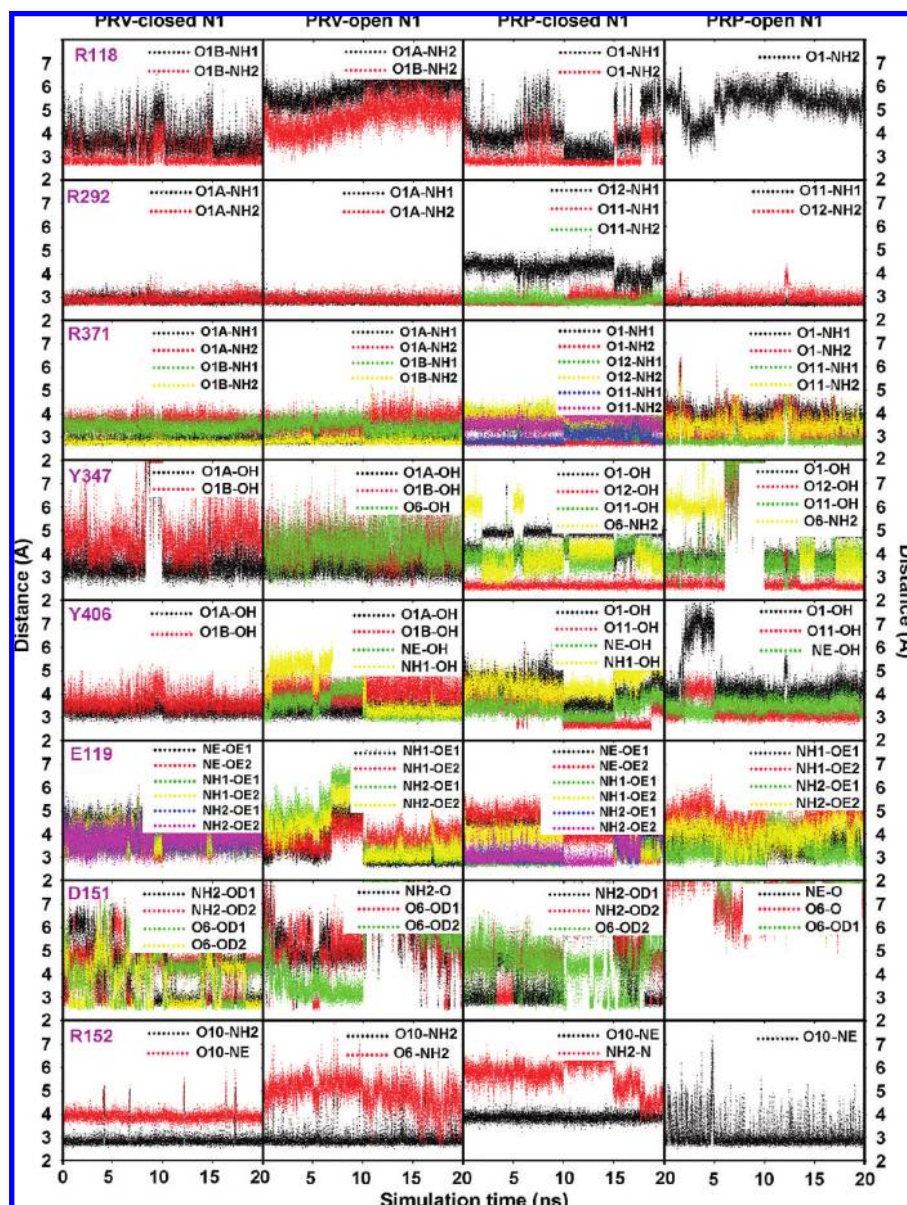


Figure 7. Time dependence of important interactions between neuraminidase N1 amino acid residues and peramivir (PRV) or its phosphonate analogue (PRP).

Although Arg152 is also located on the flexible 150-loop,¹⁴ this amino acid residue forms one firm hydrogen bond with the acetamide group of all inhibitors regardless of the neuraminidase N1 configuration. The hydrophobic groups of OTV, OTP, PRV, and PRP are incapable of forming any hydrogen-bonding interactions, while the hydrophilic group of ZNV and ZNP occasionally forms weak hydrogen bonds with various neuraminidase residues. The chloride ion of OTV-N1, ZNV-N1, and PRV-N1 systems samples random configurations as evidenced by time dependence of its distance from the simulation sphere center (Supporting Information Figure S1) and, therefore, cannot affect the obtained results in a systematic fashion.

3.3. The 150-Loop Flexibility. Our results indicate that neuraminidase N1 complexed with its inhibitor switches between open and closed conformations during the course of a 20 ns molecular dynamics simulation. Therefore, we decided to unite two independent 20 ns molecular dynamics trajectories initiated from open and closed complex configurations, respectively, into a single 40 ns trajectory (Figure

8). Free energy of the 150-loop closing down upon the bound inhibitor ΔG_{close} was subsequently determined from a standard thermodynamic relation³²

$$\Delta G_{close} = -RT \ln \left(\frac{N_{close}}{N_{open}} \right) \quad (1)$$

where R represents the universal gas constant, T is the standard temperature of 298 K, and N_{close} (N_{open}) is the number of sampled configurations with the distance between the center of the positively charged group of the inhibitor and the carboxylate carbon of Asp151 below (above) a selected threshold. The threshold selection is straightforward for OTV - average distance between the N4 atom of OTV and the carboxylate carbon of Asp151 from open (2HU0) and closed (2HU4) complex crystal structures was used (Figure 1). For comparative reasons, the analogous procedure of threshold selection was applied also for the remaining five inhibitors for which the initial open and closed complex structures were obtained by superposition. Consequently, the

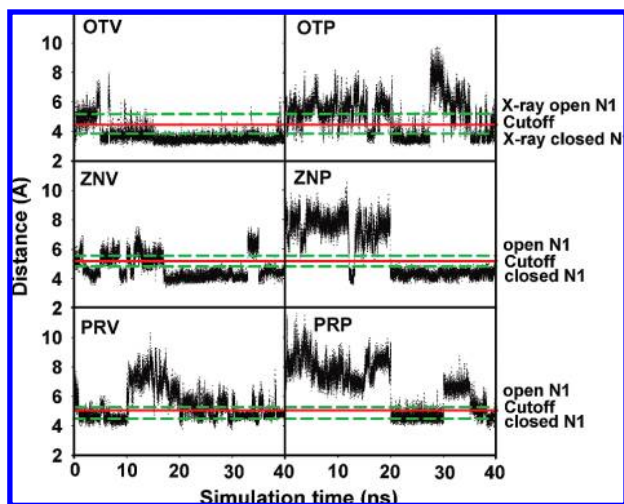


Figure 8. Time dependence of distance between the center of the positively charged group of the inhibitors (N4 atom of OTV or OTP and CZ atom of ZNV, ZNP, PRV, or PRP) and the carboxylate carbon of Asp151. The distance in the open and closed complex conformations and the selected threshold are represented by horizontal lines.

Table 3. Dependence of the Free Energy of Closing ΔG_{close} in kcal/mol upon the Threshold Selection

compound	$R_{cutoff} = 4.35 \text{ \AA}$	$R_{cutoff} = 4.55 \text{ \AA}$	$R_{cutoff} = 4.75 \text{ \AA}$
OTV	-1.14	-1.18	-1.24
OTP	0.42	0.39	0.33
compound	$R_{cutoff} = 5.05 \text{ \AA}$	$R_{cutoff} = 5.25 \text{ \AA}$	$R_{cutoff} = 5.45 \text{ \AA}$
ZNV	-0.47	-0.59	-0.76
ZNP	-0.06	-0.07	-0.07
compound	$R_{cutoff} = 4.90 \text{ \AA}$	$R_{cutoff} = 5.10 \text{ \AA}$	$R_{cutoff} = 5.30 \text{ \AA}$
PRV	0.08	-0.05	-0.15
PRP	0.55	0.46	0.40

selected thresholds were unreliable and had to be tested for the relative independence of the closing free energy ΔG_{close} upon small perturbations (0.2 Å) in the threshold distance (Table 3). Since variations in the threshold led to significant changes in the closing free energy ΔG_{close} in the case of PRV and PRP, the threshold had to be shifted toward the open structure distance for both neuraminidase N1 complexes (5.1 Å). The average distance seems not to represent the correct demarcation between open and closed complex conformations in the case of these two inhibitors, which is probably due to the occasional formation of a hydrogen bond between Asp151 and the O6 hydroxyl group of PRV or PRP.³¹

The closed complex conformation is the most favored in the case of OTV (-1.18 ± 0.06 kcal/mol), followed by ZNV (-0.6 ± 0.1 kcal/mol) and PRV (-0.1 ± 0.1 kcal/mol). The order is reversed in the case of their phosphonate congeners with ZNP (-0.07 ± 0.01 kcal/mol) followed by OTP (0.39 ± 0.06 kcal/mol) and PRP (0.46 ± 0.09 kcal/mol). Reported closing free energies indicate that the carboxylate inhibitors always prefer the closed neuraminidase N1 form more than their phosphonate analogues. This can be understood in view of the negative total charge of the phosphonate inhibitors ($-1 e_0$), which repels the Asp151 away from the inhibitor toward the open 150-loop conformation more than the zwitterionic carboxylate analogs.

4. CONCLUSIONS

Neuraminidase N1 represents an important target for rational drug design against avian influenza A (H5N1) virus as well as against currently spreading 2009 H1N1 influenza A virus. Since resistance against the existing drugs has been widely reported due to neuraminidase N1 mutations, understanding of inhibitor-neuraminidase interactions at the molecular level is of immense importance. This article reports the first comparative study of six known neuraminidase N1 inhibitors - oseltamivir, zanamivir, peramivir, and their phosphonate analogues. Their empirical force field parameters had to be developed for the application in molecular dynamics simulation of the corresponding inhibitor-neuraminidase complexes. Obtained molecular dynamics trajectories were extensively analyzed in terms of important hydrogen-bonding interactions between inhibitors and the enzyme target as well as in terms of the 150-loop flexibility. Results show that open and closed conformations of neuraminidase N1 interchange during the course of 20 ns molecular dynamics simulation for all protein-inhibitor complexes and corresponding closing free energies were determined for the first time. Phosphonate inhibitors were in comparison with their carboxylate congeners found to induce opening of the 150-loop of neuraminidase N1 - an important piece of information to assist our ongoing work toward inhibition of the H5N1 avian influenza A virus, which will be in the near future complemented by binding free energy simulations including newly designed inhibitors.

ACKNOWLEDGMENT

The work has been done under ICS-UNIDO - Thailand Universities drug discovery research program. Co-authors T.U. and T.R. would like to thank the fellowship and research grant of ICS-UNIDO. Financial support from the Slovenian Research Agency through grants P1-0002 and Z1-2000 is also gratefully acknowledged by one of the co-authors (U.B.).

Supporting Information Available: Time dependence of distance between the center of the simulated system (C2 atom of inhibitors oseltamivir (OTV), zanamivir (ZNV), and peramivir (PRV)) and the Cl^- counterion. This material is available free of charge via the Internet at <http://pubs.acs.org>.

REFERENCES AND NOTES

- (1) Oxford, J. S. Influenza A pandemics of the 20th century with special reference to 1918: virology, pathology and epidemiology. *Rev. Med. Virol.* **2000**, *10*, 119–133.
- (2) De Clercq, E. Antiviral agents active against influenza A viruses. *Nat. Rev. Drug Discovery* **2006**, *5*, 1015–1025.
- (3) Colman, P. *Structure-Based Drug Discovery: An Overview*; Royal Society of Chemistry: Cambridge, U.K., 2006.
- (4) von Itzstein, M.; Wu, W.-Y.; Kok, G. B.; Pegg, M. S.; Dyason, J. C.; J., Betty; van Phan, T.; Smythe, M. L.; White, H. F.; Oliver, S. W.; Colman, P. M.; Varghese, J. N.; Ryan, D. M.; Woods, J. M.; Bethell, R. C.; Hotham, V. J.; Cameron, J. M.; Penn, C. R. Rational design of potent sialidase-based inhibitors of influenza virus replication. *Nature* **1993**, *363*, 418–423.
- (5) Kim, C. U.; Lew, W.; Williams, M. A.; Liu, H.; Zhang, L.; Swaminathan, S.; Bischofberger, N.; Chen, M. S.; Mendel, D. B.; Tai, C. Y.; Laver, W. G.; Stevens, R. C. Influenza neuraminidase inhibitors possessing a novel hydrophobic interaction in the enzyme active site: Design, synthesis, and structural analysis of carbocyclic sialic acid

- analogues with potent anti-influenza activity. *J. Am. Chem. Soc.* **1997**, *119*, 681–690.
- (6) Bantia, S.; Arnold, C. S.; Parker, C. D.; Upshaw, R.; Chand, P. Anti-influenza virus activity of peramivir in mice with single intramuscular injection. *Antiviral Res.* **2006**, *69*, 39–45.
 - (7) Chand, P.; Bantia, S.; Kotian, P.; El-Kattan, Y.; Lin, T.; Babu, Y. S. Comparison of the anti-influenza virus activity of cyclopentane derivatives with oseltamivir and zanamivir in vivo. *Bioorg. Med. Chem.* **2005**, *13*, 4071–4077.
 - (8) Ward, P.; Small, I.; Smith, J.; Suter, P.; Dutkowski, R. Oseltamivir (Tamiflu) and its potential for use in the event of an influenza pandemic. *J. Antimicrob. Chemother.* **2005**, *55*, 5–21.
 - (9) Le, Q. M.; Kiso, M.; Someya, K.; Sakai, Y. T.; Nguyen, T. H.; Nguyen, K. H. L.; Pham, N. D.; Ngyen, H. H.; Yamada, S.; Muramoto, Y.; Horimoto, T.; Takada, A.; Goto, H.; Suzuki, T.; Suzuki, Y.; Kawaoka, Y. Avian flu: isolation of drug-resistant H5N1 virus. *Nature* **2005**, *43*, 1108.
 - (10) Kiso, M.; Mitamura, K.; Sakai-Tagawa, Y.; Shiraishi, K.; Kawakami, C.; Kimura, K.; Hayden, F.; Sugaya, N.; Kawaoka, Y. Resistant influenza A viruses in children treated with oseltamivir: descriptive study. *Lancet* **2004**, *364*, 759–765.
 - (11) de Jong, M. D.; Tran, T. T.; Truong, H. K.; Vo, M. H.; Smith, G. J.; Nguyen, V. C.; Bach, V. C.; Phan, T. Q.; Do, Q. H.; Guan, Y.; Peiris, J. S.; Tran, T. H.; Farrar, J. Oseltamivir resistance during treatment of influenza A (H5N1) infection. *N. Engl. J. Med.* **2005**, *353*, 2667–2672.
 - (12) Shie, J. -J.; Fang, J. -M.; Wang, S. -Y.; Tsai, K. -C.; Cheng, Y. -S. E.; Yang, A. -S.; Hsiao, S. -C.; Su, C. Y.; Wong, C. -H. Synthesis of Tamiflu and its phosphonate congeners possessing potent anti-influenza activity. *J. Am. Chem. Soc.* **2007**, *129*, 11892–11893.
 - (13) Russell, R. J.; Haire, L. F.; Stevens, D. J.; Collins, P. J.; Lin, Y. P.; Blackburn, G. M.; Hay, A. J.; Gamblin, S. J.; Skehel, J. J. The structure of H5N1 avian influenza neuraminidase suggests new opportunities for drug design. *Nature* **2006**, *443*, 45–49.
 - (14) Amaro, R. E.; Minh, D. D.; Cheng, L. S.; Lindstrom, W. M., Jr.; Olson, A. J.; Lin, J. H.; Li, W. W.; McCammon, J. A. Remarkable loop flexibility in avian influenza N1 and its implications for antiviral drug design. *J. Am. Chem. Soc.* **2007**, *129*, 7764–7765.
 - (15) Zhang, Q.; Yang, J.; Liang, K.; Feng, L.; Li, S.; Wan, J.; Xu, X.; Yang, G.; Liu, D.; Yang, S. Binding Interaction Analysis of the Active Site and Its Inhibitors for Neuraminidase (N1 Subtype) of Human Influenza Virus by the Integration of Molecular Docking, FMO Calculation and 3D-QSAR CoMFA Modeling. *J. Chem. Inf. Model.* **2008**, *48*, 1802–1812.
 - (16) Borštnik, U.; Hodošček, M.; Janežič, D. Improving the performance of molecular dynamics simulations on parallel clusters. *J. Chem. Inf. Comput. Sci.* **2004**, *44*, 359–364.
 - (17) Borštnik, U.; Janežič, D. Symplectic molecular dynamics simulations on specially designed parallel computers. *J. Chem. Inf. Model.* **2005**, *45*, 1600–1604.
 - (18) Marelus, J.; Kolmodin, K.; Feierberg, I.; Åqvist, J. Q. A molecular dynamics program for free energy calculations and empirical valence bond simulations in biomolecular systems. *J. Mol. Graphics Modell.* **1998**, *16*, 213–225.
 - (19) Cornell, W. D.; Cieplak, P.; Bayly, C. I.; Gould, I. R.; Merz, K. M., Jr.; Ferguson, D. M.; Spellmeyer, D. C.; Fox, T.; Caldwell, J. W.; Kollman, P. A. A second generation force field for the simulation of proteins, nucleic acids, and organic molecules. *J. Am. Chem. Soc.* **1995**, *117*, 5179–5197.
 - (20) Jorgensen, W. L.; Chandrasekhar, J.; Madura, J. D.; Impey, R. W.; Klein, M. L. Comparison of simple potential functions for simulating liquid water. *J. Chem. Phys.* **1983**, *79*, 926–935.
 - (21) King, G.; Warshel, A. A surface constrained all-atom solvent model for effective simulations of polar solutions. *J. Chem. Phys.* **1989**, *91*, 3647–3661.
 - (22) Lee, F. S.; Warshel, A. A local reaction field method for fast evaluation of long-range electrostatic interactions in molecular simulations. *J. Chem. Phys.* **1992**, *97*, 3100–3107.
 - (23) Ryckaert, J. -P.; Ciccotti, G.; Berendsen, H. J. C. Numerical integration of the cartesian equations of motion of a system with constraints: molecular dynamics of n-alkanes. *J. Comput. Phys.* **1977**, *23*, 327–341.
 - (24) van Gunsteren, W. F.; Berendsen, H. J. C. Algorithms for macromolecular dynamics and constraint dynamics. *Mol. Phys.* **1977**, *34*, 1311–1327.
 - (25) Humphrey, W.; Dalke, A.; Schulten, K. VMD: visual molecular dynamics. *J. Mol. Graph.* **1996**, *14*, 33–38.
 - (26) Frisch, M. J.; Trucks, G. W.; Schlegel, H. B.; Scuseria, G. E.; Robb, M. A.; Cheeseman, J. R.; Montgomery, J. A., Jr.; Vreven, T.; Kudin, K. N.; Burant, J. C.; Millam, J. M.; Iyengar, S. S.; Tomasi, J.; Barone, V.; Mennucci, B.; Cossi, M.; Scalmani, G.; Rega, N.; Petersson, G. A.; Nakatsuji, H.; Hada, M.; Ehara, M.; Toyota, K.; Fukuda, R.; Hasegawa, J.; Ishida, M.; Nakajima, T.; Honda, Y.; Kitao, O.; Nakai, H.; Klene, M.; Li, X.; Knox, J. E.; Hratchian, H. P.; Cross, J. B.; Bakken, V.; Adamo, C.; Jaramillo, J.; Gomperts, R.; Stratmann, R. E.; Yazyev, O.; Austin, A. J.; Cammi, R.; Pomelli, C.; Ochterski, J. W.; Ayala, P. Y.; Morokuma, K.; Voth, G. A.; Salvador, P.; Dannenberg, J. J.; Zakrzewski, V. G.; Dapprich, S.; Daniels, A. D.; Strain, M. C.; Farkas, O.; Malick, D. K.; Rabuck, A. D.; Raghavachari, K.; Foresman, J. B.; Ortiz, J. V.; Cui, Q.; Baboul, A. G.; Clifford, S.; Cioslowski, J.; Stefanov, B. B.; Liu, G.; Liashenko, A.; Piskorz, P.; Komaromi, I.; Martin, R. L.; Fox, D. J.; Keith, T.; Al-Laham, M. A.; Peng, C. Y.; Nanayakkara, A.; Challacombe, M.; Gill, P. M. W.; Johnson, B.; Chen, W.; Wong, M. W.; Gonzalez, C.; Pople, J. A. *Gaussian 03, Revision C.02*; Gaussian, Inc.: Wallingford, CT, 2004.
 - (27) Bren, U.; Hodošček, M.; Koller, J. Development and Validation of Empirical Force Field Parameters for Netropsin. *J. Chem. Inf. Model.* **2005**, *45*, 1546–1552.
 - (28) Bayly, C. I.; Cieplak, P.; Cornell, W. D.; Kollman, P. A. A Well-Behaved Electrostatic Potential Based Method Using Charge Restraints for Deriving Atomic Charges: The RESP Model. *J. Phys. Chem.* **1993**, *97*, 10269–10280.
 - (29) Wang, J.; Wolf, R. M.; Caldwell, J. W.; Kollman, P. A.; Case, D. A. Development and testing of a general AMBER force field. *J. Comput. Chem.* **2004**, *25*, 1157–1174.
 - (30) Rungrotmongkol, T.; Frece, V.; De-Eknamkul, W.; Hannongbua, S.; Miertus, S. Design of oseltamivir analogs inhibiting neuraminidase of avian influenza virus H5N1. *Antiviral Res.* **2009**, *82*, 51–58.
 - (31) Malaisree, M.; Rungrotmongkol, T.; Decha, P.; Intharathep, P.; Aruksakunwong, O.; Hannongbua, S. Understanding of known drug-target interactions in the catalytic pocket of neuraminidase subtype N1. *Proteins: Struct., Funct., Bioinf.* **2008**, *71*, 1908–1918.
 - (32) Martinek, V.; Bren, U.; Goodman, M. F.; Warshel, A.; Florian, J. DNA polymerase β catalytic efficiency mirrors the Asn279-dCTP H-bonding strength. *FEBS Lett.* **2007**, *581*, 775–780.

CI900277R